IOPscience iopscience.iop.org

Home Search Collections Journals About Contact us My IOPscience

Electronic structure of the misfit layer compound $(LaS)_{1.14}NbS_2$: band-structure calculations and photoelectron spectra

This article has been downloaded from IOPscience. Please scroll down to see the full text article.

1996 J. Phys.: Condens. Matter 8 5367

(http://iopscience.iop.org/0953-8984/8/29/012)

View the table of contents for this issue, or go to the journal homepage for more

Download details:
IP Address: 171.66.16.206
The article was downloaded on 13/05/2010 at 18:20

Please note that terms and conditions apply.

J. Phys.: Condens. Matter **8** (1996) 5367–5382. Printed in the UK

Electronic structure of the misfit layer compound $(LaS)_{1.14}NbS_2$: band-structure calculations and photoelectron spectra

C M Fang, S van Smaalen†, G A Wiegers, C Haas and R A de Groot

Laboratory of Chemical Physics, Materials Science Center, University of Groningen, Nijenborg 4, 9747 AG Groningen, The Netherlands

Received 11 March 1996

Abstract. In order to understand the electronic structure of the misfit layer compound $(LaS)_{1.14}NbS_2$ we carried out an *ab initio* band-structure calculation in a supercell approximation. The band structure is compared with that of the components NbS_2 and LaS. The calculations show that the electronic structure of $(LaS)_{1.14}NbS_2$ can be regarded as that of LaS intercalated into the host NbS_2. There is a transfer of about 0.7 electrons per Nb atom from the LaS to the NbS_2 layers; some electrons remain in La 5d orbitals. The states at the Fermi level are dominated by Nb $4d_{z^2}$ orbitals; there are about 0.3 holes per Nb atom. The dispersion of the energy bands shows a large anisotropy. The dispersion of energy bands for the LaS subsystem is very small along the incommensurate direction. X-ray and ultraviolet photoelectron spectra obtained for the core level electrons and the valence bands are in good agreement with the band-structure calculations.

1. Introduction

Misfit layer compounds have the general formula $(MX)_{1+x}(TX_2)_m$ (M = Sn, Pb, Bi, Sb or rare-earth metal; X = S or Se; T = Ti, V, Cr, Nb or Ta; $0.08 < x < 0.26$; $m = 1, 2$) and planar intergrowth structures [1–3]. They are build of alternating double layers MX and sandwiches TX_2, which do not match. These compounds therefore lack three-dimensional periodicity. The stability of the misfit layer compounds, the interlayer chemical bonding and the effect of the incommensurateness on their physical properties are subjects of interest.

The band-structure calculations of $(SnS)_{1.17}NbS_2$ and $(SnS)_{1.20}TiS_2$ showed that the electronic structure is approximately a superposition of the electronic structures of the components TX_2 and MX with a small charge transfer from the MX layer to the TX_2 layers. The interlayer interaction between MX and TX_2 is dominated by covalent interactions [4, 5].

However, for the rare-earth-metal-based misfit layer compounds there are some differences. The in-plane resistivity, Hall coefficient and thermopower measurements of the rare-earth-metal-based compounds show p-type metallic conduction, which prompted the suggestion that the conduction was by holes in the d_{z^2} band of the NbS_2 or TaS_2 sandwiches [1–3]. This d_{z^2} band, which may contain two electrons per T = Nb or Ta and is half filled in the case of pure dichalcogenides 2H-NbS_2 and 2H-TaS_2, is filled to 0.1–0.3 holes per T in the case of the rare-earth misfit layer compounds.

† Present address: Laboratory of Crystallography, University of Bayreuth, D95440 Bayreuth, Germany.

0953-8984/96/295367+16$19.50 © 1996 IOP Publishing Ltd

So far there have been no reports on electronic structure calculations for rare-earth-based misfit layer compounds. This paper reports the results of band-structure calculations in the supercell approximation and photoelectron spectra (x-ray photoelectron spectroscopy (XPS) and ultraviolet photoelectron spectroscopy (UPS)) for the core levels and the valence bands of the misfit layer compound $(LaS)_{1.14}NbS_2$. The origin of the stability and the interlayer chemical bonding of $(LaS)_{1.14}NbS_2$ and other rare-earth-metal-based misfit layer compounds are discussed.

2. Structure of $(LaS)_{1.14}NbS_2$

$(LaS)_{1.14}NbS_2$ has been synthesized by Meerschaut *et al* [6]. However, they determined the structure in a supercell with a wrong space group. Wiegers *et al* [7] determined the structure in the composite structure approach, which means that separate refinements were carried out for the LaS substructure with unit-cell dimensions $a_1 = 5.818$ Å, $b_1 = 5.797$ Å and $c_1 = 11.512$ Å, space group $Cm2a$ and $Z = 4$, for the NbS_2 part with $a_2 = 3.310$ Å, $b_2 = 5.797$ Å and $c_2 = 23.04$ Å, space group $Fm2m$ and $Z = 4$, and the common projection along [100] (reflections $0kl$) which determines the relative position along [010] and [001] of the two subsystems. The in-plane axes are a and b. The b axes are parallel and of equal length, while the a axes, being parallel, have a length ratio $a_1/a_2 = 5.818/3.310 \simeq 1.758$, being close to 7/4 (= 1.75). The c axes are parallel but c for NbS_2 is twice the c for LaS because of the F centring of the NbS_2 lattice (figure 1). The coordinates of the atoms in the unit cells of the two subsystems are given in table 1 [7]. The LaS part of the structure consists of double layers, resembling slices of solid LaS (NaCl-type structure, $a = 5.834$ Å) with a thickness of half the cell edge. The LaS double layer is corrugated with the La atoms on the outside, making possible bonding interactions with the sulphur atoms of NbS_2 layers. Each La atom is coordinated to five S atoms in the double layer and to one or two S atoms of the neighbouring NbS_2 layer. The NbS_2 sandwiches are about the same as in 2H-NbS_2, Nb atoms being in approximately a trigonal prism of S atoms. The two substructures mutually modulate each other incommensurately. The complete structure, including the modulation is described in a (3+1)-dimensional superspace group [2, 8]. The modulation amplitudes were determined by van Smaalen [8] using the program system JANA [9]. The refinement in JANA showed that the largest modulation amplitudes are for the La atoms and the S atoms of the NbS_2 layers [8]. The program system JANA allows one to approximate the incommensurate structure in a supercell as needed for a band-structure calculation, the smallest being that with $a = 7a_2 \simeq 4a_1$ (= 23.216 Å), $b = b_1 = b_2$ (= 5.806 Å), and $c = 2c_1 = c_2$ (= 23.03 Å). Several choices are possible for the space group depending on the choice of the origin along the incommensurate axis of one subsystem with respect to the other. The supercell with the highest symmetry was chosen, since it gives the smallest number of crystallographically independent atoms. The structure described here is the ideal structure and does not contain vacancies on the La sites as suggested by Wiegers [3], analogous to the La vacancies in '$LaCrS_3$', '$GdCrS_3$' and '$YCrS_3$' suggested by Rouxel *et al* [10] and Lafond *et al* [11], and in '$LaVSe_3$' suggested by Ren *et al* [12].

The supercell with the highest symmetry deduced from JANA has the space group $Ccc2$ and unit-cell dimensions $a = 23.03$ Å, $b = 23.216$ Å (= $7a_2 \simeq 4a_1$) and $c = 5.806$ Å (figure 2). Note that this choice is the standard setting according to [13]. The cell content is $(LaS)_{32}(NbS_2)_{28}$. All atoms are on general sites 8d, except Nb(1) which is on site 4c (see table 4 later). The crystallographically independent atoms are therefore reduced to four Nb, four La and 11 S atoms. The intralayer and interlayer La–S distances for the four independent La atoms are given in table 2; those for the average structure (the mutual

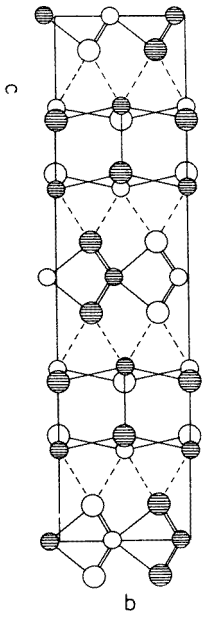

Figure 1. [100] projection of the unmodulated (average) structure of $(LaS)_{1.14}NbS_2$. The small circles are Nb and La atoms (Nb at $z = 0$ and $\frac{1}{2}$), and the large circle are S atoms. Atoms of the same subsystem $a/2$ apart are indicated by open and filled-circles of the same size. Broken lines indicate the interaction of La with S of the NbS_2 layer.

Table 1. Atomic coordinates in the unit cells of the subsystems LaS (space group, $Cm2a$) and NbS_2 (space group, $Fm2m$) of $(LaS)_{1.14}NbS_2$. WP is the Wyckoff position.

LaS	WP	x	y	z	NbS_2	WP	x	y	z
La	4(c)	$\frac{1}{4}$	0	0.6527	Nb	4(a)	0.0	−0.0750	0.0
S(1)	4(c)	$\frac{1}{4}$	0.504	0.6009	S(2)	8(c)	0.0	0.258	0.0679

modulation not taken into account) are also included.

Some insight into the bonding can be obtained by using the concept of bond valence [14]. The bond valence V_i is calculated from the relation $V_i = \exp[(d_0 - d_i)/b]$, where d_i is the distance between the atoms of bond i, and d_0 and b are empirical constants: $d_0 = 2.64$ Å for La–S and $b = 0.37$ Å [15]. The bond valence or oxidation state V of an atom is calculated by summing over all neighbouring atoms $V = \sum_i V_i$. For comparison the La–S distances [16] and bond valences of LaS and La_2S_3 are given in table 3.

The intralayer La–S bond valences vary from 1.9 to 2.3 valence units (vu) for different La atoms. The interlayer La–S bond valences are quite large (0.80–0.96 vu) in contrast with the interlayer M–S bond valences in the misfit layer compounds $(MX)_nTX_2$ with M = Sn or Bi [3–5]. The sum of the La bond valence is about +3.

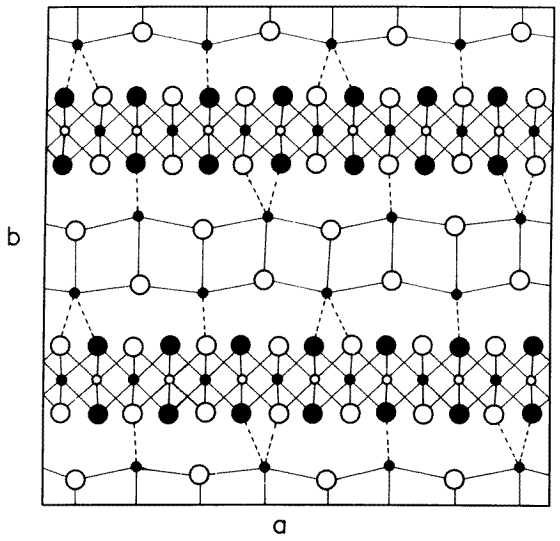

Figure 2. Projection of the unit cell of $(LaS)_{1.14}NbS_2$ along [001] in the large supercell, of space group $Ccc2$. Seven unit cells of NbS_2 correspond to four unit cells of LaS. The large circles are S atoms of the NbS_2 layers with the open and full circles for $z \simeq \frac{1}{4}$ and $z \simeq \frac{3}{4}$, respectively, and of the LaS layers with $z \simeq 0$. The open and full small circles ($y \simeq \frac{1}{4}$ and $y \simeq \frac{3}{4}$) represent the Nb atoms at $z \simeq 0.0$ and $z \simeq \frac{1}{2}$, respectively. The small full circles near $y \simeq 0$ and $y \simeq \frac{1}{2}$ represent the La atoms ($z \simeq 0.0$). The La and S atoms at $z \simeq \frac{1}{2}$ of the LaS layers are not indicated for clarity.

Table 2. Interatomic distances d_i and bond valences V_i in the modulated structure, of space group $Ccc2$, of $(LaS)_{1.14}NbS_2$; a and b are intralayer and interlayer La–S bonds, respectively. La* is the average structure. The numbering of the La atoms corresponds to table 4.

	La(1)		La(2)		La(3)		La(4)		La*	
	d_i (Å)	V_i	d_i (Å)	V_i	d_i (Å)	V_i	d_i (Å)	V_i	d_i (Å)	V_i
a	2.901	0.494	3.092	0.295	2.934	0.452	2.876	0.528	2.990	0.388
a	3.015	0.363	2.846	0.573	3.022	0.356	3.039	0.340	2.940	0.444
a	2.846	0.573	3.028	0.350	3.047	0.333	3.037	0.342	2.963	0.418
a	2.982	0.397	2.956	0.426	3.047	0.333	2.877	0.527	2.963	0.418
a	2.928	0.459	2.914	0.477	2.940	0.444	2.904	0.417	2.921	0.468
$V_a = \sum_i V_i$		2.29		2.12		1.92		2.15		2.14
b	3.309	0.164	2.988	0.390	3.108	0.282	3.087	0.299		
b	3.182	0.231	2.975	0.405	3.257	0.189	3.585	0.078		
b	2.897	0.499	3.554	0.085	2.904	0.490	2.902	0.419		
$V_b = \sum_i V_i$		0.89		0.88		0.96		0.80		
V_{total}		3.18		3.00		2.88		2.95		

3. Band-structure calculations

3.1. Method of the calculations

Ab-initio band-structure calculations were performed with the localized spherical wave

Table 3. Interatomic distances d_i and bond valences V_i in LaS and La_2S_3 [13].

		La_2S_3			
LaS		La(1)		La(2)	
d_i (Å)	V_i	d_i (Å)	V_i	d_i (Å)	V_i
6 × 2.917	0.473	2.94	0.444	3.16	0.245
		3.045	0.335	3.17	0.239
		3.050	0.330	2×3.07	0.312
		2×2.95	0.433	2×2.91	0.482
		2×2.91	0.482	2×3.045	0.335
$V = \sum_i V_i$	2.84		2.94		2.74

(LSW) method [17] using a scalar-relativistic Hamiltonian. We used local-density exchange–correlation potentials [18] inside space filling, and therefore overlapping spheres around the atomic constituents. The self-consistent calculations were carried out including all core electrons.

Iterations were performed with $\boldsymbol{k}$-points distributed uniformly in an irreducible part of the first Brillouin zone (BZ), corresponding to a volume per $\boldsymbol{k}$-point of the order of 1.5×10^{-5} Å^{-3}. Self-consistency was assumed when the changes in the local partial charges in each atomic sphere decreased to the order of 10^{-5}.

In the construction of the LSW basis [17, 19], the spherical waves were augmented by solutions of the scalar-relativistic radial equations indicated by the atomic symbols 6s, 6p, 5d corresponding to the valence levels of the parent elements La, 5s, 5p, 4d to Nb and 3s, 3p, 3d to S. The internal l summation used to augment a Hankel function at surrounding atoms was extended to $l = 3$, resulting in the use of 4f orbitals for La and Nb. When the crystal is not very densely packed, as is the case in layered materials such as $(LaS)_{1.14}NbS_2$, it is necessary to include empty spheres in the calculations. The functions 1s and 2p, and 3d as an extension, were used for the empty spheres. The input parameters (lattice constants, atomic coordinates, and Wigner–Seitz sphere radii of atoms and empty spheres) are listed in table 4.

3.2. The densities of states of the components LaS and NbS$_2$

For a better understanding of the band structure of $(LaS)_{1.14}NbS_2$ it is useful to compare the results of the calculations with band structures of the two components LaS and NbS_2.

We calculated the band structure of LaS by the LSW method. The input parameters for band-structure calculations of LaS are given in table 5. The electronic structure agrees with the results of Lu *et al* [20]. The density of states (DOS) of LaS is shown in figure 3. The sulphur 3s states are clearly separated from the other states of the valence band by a gap of 7.1 eV. The next band consists mainly of S 3p states slightly hybridized with La 5d orbitals. The La 5d band is very broad; it begins at −2.6 eV and is separated from the S 3p band by an energy gap of 0.7 eV. The hybridization of La 5d, 6s, 6p states with S 3p orbitals is small. The bonding is therefore rather ionic. The Fermi level is in the La 5d bands; there is one 5d electron per La atom which is responsible for the metallic electrical conduction of LaS. The La 4f states are calculated at about 3.5 eV above the Fermi energy. However, it is well known that local-density band-structure calculations give an energy for unoccupied 4f states of La which is about 5 eV too low [21].

Table 4. Coordinates of the atoms and empty spheres, and the Wigner–Seitz radii R_{WS} used for the band-structure calculation of $(LaS)_{1.14}NbS_2$ in the supercell with $a = 23.216$ Å, $b = 23.03$ Å and $c = 5.806$ Å, and of space group $Ccc2$. WP is the Wyckoff position.

Atom	WP	Coordinates	R_{WS} (Å)
Nb(1)	4c	(0.2500, 0.2500, 0.5718)	1.2483
Nb(2)	8d	(0.0368, 0.2496, 0.0736)	1.2483
Nb(3)	8d	(0.6062, 0.2498, 0.0723)	1.2483
Nb(4)	8d	(0.1791, 0.2505, 0.0745)	1.2483
S(1)	8d	(0.0332, 0.3188, −0.2558)	1.7216
S(2)	8d	(0.1780, 0.3156, −0.2549)	1.6644
S(3)	8d	(0.6097, 0.3192, −0.2631)	1.7216
S(4)	8d	(0.4653, 0.3166, −0.2596)	1.7164
S(5)	8d	(0.3225, 0.3184, −0.2502)	1.7216
S(6)	8d	(0.8925, 0.3180, −0.2652)	1.7216
S(7)	8d	(0.7488, 0.3190, −0.2670)	1.7216
La(1)	8d	(0.3147, 0.5758, −0.0182)	1.5334
La(2)	8d	(0.5591, 0.5762, 0.0093)	1.5344
La(3)	8d	(0.8154, 0.5780, 0.0123)	1.5344
La(4)	8d	(0.0608, 0.5752, −0.0033)	1.5344
S(8)	8d	(0.3129, 0.5512, −0.5082)	1.9263
S(9)	8d	(0.5654, 0.5500, −0.5124)	1.9055
S(10)	8d	(0.8101, 0.5494, −0.4956)	1.9263
S(11)	8d	(0.0607, 0.5508, −0.5176)	1.9263
Va(1)	4a	(0.0000, 0.0000, −0.2590)	0.9570
Va(2)	4b	(0.0000, 0.5000, −0.2676)	0.8998
Va(3)	8d	(0.1262, 0.0000, −0.2624)	0.8790
Va(4)	8d	(0.6249, 0.0000, −0.2550)	0.8946
Va(5)	8d	(0.2490, 0.0000, −0.2501)	0.8738
Va(6)	4c	(0.2500, 0.2500, −0.9700)	1.0767
Va(7)	8d	(0.5338, 0.2420, −0.0963)	1.0663
Va(8)	8d	(0.1080, 0.2500, −0.0960)	1.0741
Va(10)	8d	(0.6785, 0.2505, −0.0915)	1.0637
Va(11)	8d	(0.1252, 0.1220, −0.0090)	0.6814
Va(12)	8d	(0.7490, 0.1240, 0.0000)	0.7230

Table 5. Input parameters for band-structure calculations of LaS ($a = 5.834$ Å; space group, $Fm\bar{3}m$) and electronic configuration obtained. WP is the Wyckoff position.

	WP	Coordinates x	y	z	R_{WS} (Å)	Electronic configuration
La	1a	0	0	0	1.4213	$[Xe]5d^{0.51}6s^{0.06}6p^{0.12}4f^{0.11}$
S	1b	$\frac{1}{2}$	$\frac{1}{2}$	$\frac{1}{2}$	2.0831	$[Ne]3s^{1.96}3p^{5.35}3d^{0.78}\ 4f^{0.10}$

Several good band-structure calculations are available for 2H-NbS_2 [4, 22]. In order to compare with the band structure of the misfit layer compound we have calculated the band structure of 2H-NbS_2 using the LSW method [4]. The total and partial DOSs are shown in figure 4. The band structure obtained for 2H-NbS_2 is similar to previous calculations.

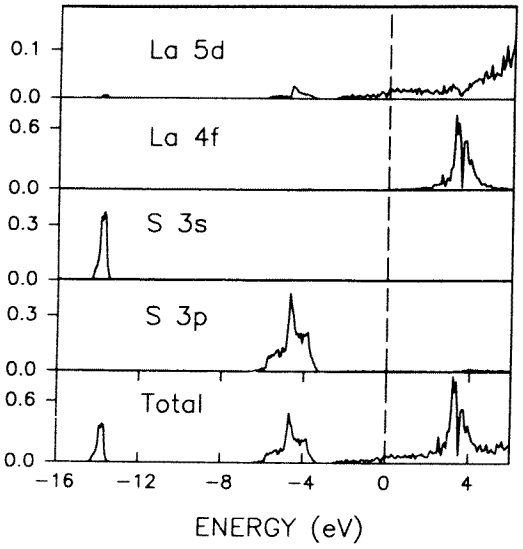

Figure 3. The total and partial DOSs of LaS.

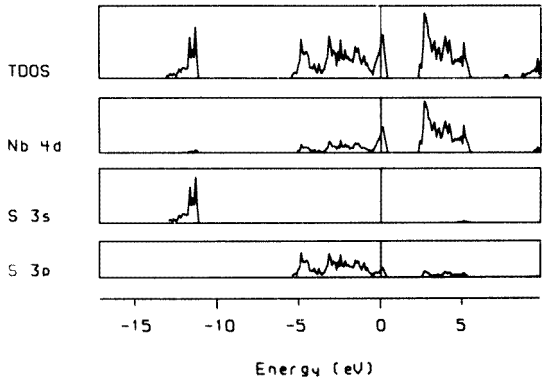

Figure 4. Total and partial DOSs of 2H-NbS_2.

3.3. Band structure of $(LaS)_{1.14}NbS_2$

The first BZ corresponding to the large unit cell with space group $Ccc2$ (No. 37) is shown in figure 5. The dispersions of the energy bands near the Fermi level and of the sulphur 3s state band are shown in figures 6(a) and 6(b) for selected directions in the BZ. The total and partial DOSs obtained from the band-structure calculations are shown in figure 7. The orbital configurations of atoms and empty spheres are given in table 6. We remark that not too much significance should be attributed to differences in charge and orbital configuration, as these numbers are strongly dependent on the Wigner–Seitz radii, and the presence of empty spheres. However, we observe that the variation in the electronic configuration of one type of atom within a subsystem is small; this indicates that the modulation of the electronic structure of one subsystem by the other subsystem is small. There is a small but significant

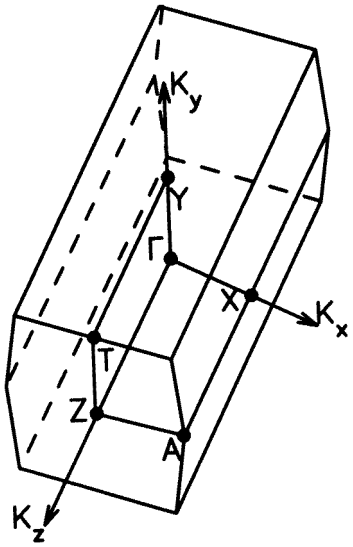

Figure 5. BZ and high-symmetry points of $(LaS)_{1.14}NbS_2$ with space group $Ccc2$.

difference between the electronic configurations of S in the NbS_2 and the LaS subsystems, but this is at least partly due to the different Wigner–Seitz radii.

Table 6. Electronic configurations of the atoms in $(LaS)_{1.14}NbS_2$.

Atom	Electronic configuration
NbS_2 subsystem	
Nb(1)	$[Kr]4d^{2.16}5s^{0.14}5p^{0.20}4f^{0.03}$
Nb(2)	$[Kr]4d^{2.07}5s^{0.15}5p^{0.21}4f^{0.04}$
Nb(3)	$[Kr]4d^{2.13}5s^{0.15}5p^{0.20}4f^{0;04}$
Nb(4)	$[Kr]4d^{2.09}5s^{0.15}5p^{0.22}4f^{0.04}$
S(1)	$[Ne]3s^{1.92}3p^{5.00}3d^{0.24}$
S(2)	$[Ne]3s^{1.89}3p^{4.89}3d^{0.22}$
S(3)	$[Ne]3s^{1.91}3p^{4.99}3d^{0.24}$
S(4)	$[Ne]3s^{1.91}3p^{5.02}3d^{0.25}$
S(5)	$[Ne]3s^{1.91}3p^{4.94}3d^{0.25}$
S(6)	$[Ne]3s^{1.91}3p^{5.04}3d^{0.26}$
S(7)	$[Ne]3s^{1.92}3p^{4.98}3d^{0.25}$
LaS subsystem	
La(1)	$[Xe]5d^{0.52}6s^{0.09}6p^{0.14}4f^{0.15}$
La(2)	$[Xe]5d^{0.56}6s^{0.09}6p^{0.14}4f^{0.15}$
La(3)	$[Xe]5d^{0.68}6s^{0.13}6p^{0.17}4f^{0.16}$
La(4)	$[Xe]5d^{0.55}6s^{0.09}6p^{0.15}4f^{0.15}$
S(8)	$[Ne]3s^{1.95}3p^{5.14}3d^{0.16}$
S(9)	$[Ne]3s^{1.94}3p^{5.17}3d^{0.13}$
S(10)	$[Ne]3s^{1.97}3p^{5.02}3d^{0.14}$
S(11)	$[Ne]3s^{1.95}3p^{5.15}3d^{0.22}$

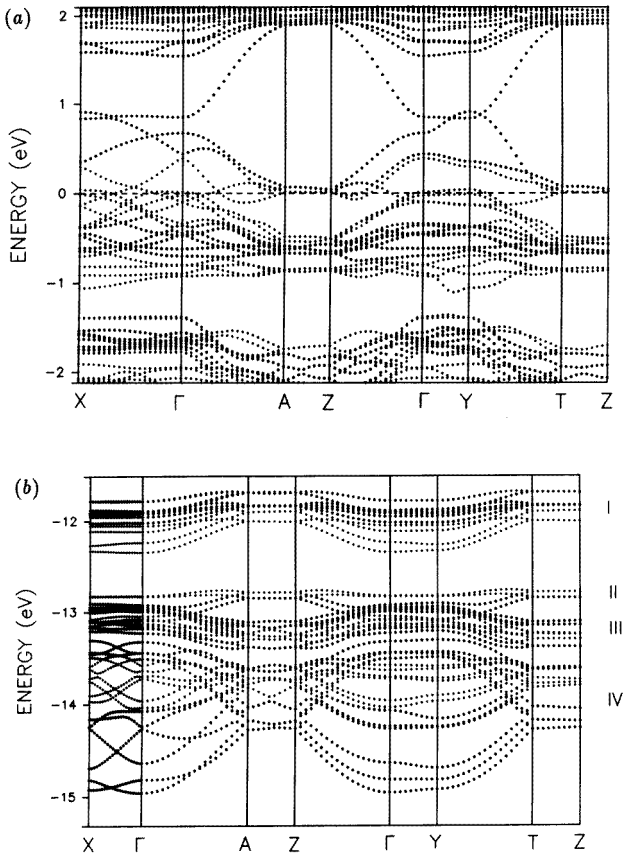

Figure 6. (*a*) Dispersion of the energy bands near the Fermi level for $(LaS)_{1.14}NbS_2$. (*b*) Dispersion of the energy bands of S 3s states for $(LaS)_{1.14}NbS_2$. The bands I–IV are discussed in the text.

In the total DOS we can distinguish two separate sets of energy bands. The lowest bands mainly consist of sulphur 3s orbitals, with in the lower part mainly S 3s of the NbS_2 subsystem, whereas the S 3s states of the LaS subsystem are at the top of these bands. There is a shift of about 1.2 eV to a lower energy of the top of S 3s band of the NbS_2 subsystem in the misfit layer compound with respect to the Fermi level, compared with 2H-NbS_2. Part of the shift will be due to the higher Fermi energy in the $(LaS)_{1.14}NbS_2$ compound, as a result of increased filling of the Nb $4d_{z^2}$ band. Part of the shift could be due to a lowering of the S 3s orbital energy by the Coulomb interaction with La. Most of the S 3s bands of the LaS subsystem shift to higher energy with respect to the Fermi level, compared with LaS. These shifts are at least partly explained by the high Fermi level in LaS, due to the presence of 1 electron per La atom in the broad La 5d band.

The energy gap between the S 3s and the S 3p states is about 3.4 eV, which is smaller than for 2H-NbS_2 (about 6.10 eV) and for LaS (about 7.1 eV). The bands between −8.15 and −1.40 eV are S 3p bands hybridized with some La 5d and Nb 4d states. The S 3p states of the NbS_2 subsystem hybridized with Nb 4d orbitals spread over the whole band, while the S 3p of the LaS subsystem hybridized with La 5d states are in the upper part of

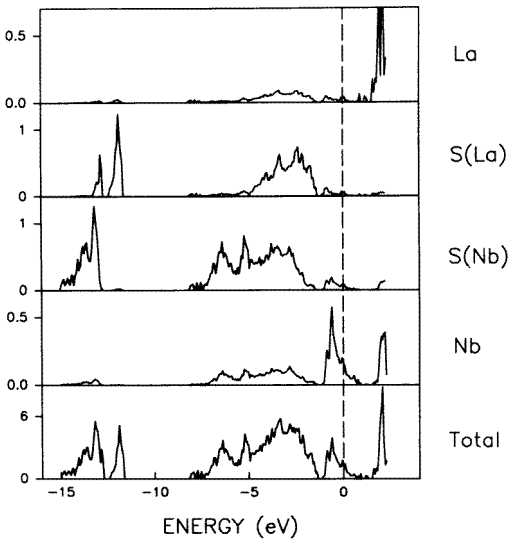

Figure 7. Total and partial DOSs of $(LaS)_{1.14}NbS_2$; S atoms in the LaS and NbS_2 subsystems are indicated as S(La) and S(Nb), respectively.

the band. The band ranging from −1.1 to 1.0 eV consists mainly of Nb 4d-($4d_{z^2}$) states hybridized with some S 3p and La 5d orbitals. This Nb $4d_{z^2}$ band contains about 0.3 holes per Nb atom. This indicates that there is a transfer of about 0.7 electrons per Nb atom from the LaS to the NbS_2 layers because in 2H-NbS_2 the Nb $4d_{z^2}$ band is half occupied and contains one hole per Nb atom.

Figures 6(a) and 6(b) show the dispersion curves for selected directions in the BZ. The S 3s states form three parts. The 12 top bands (I in figure 6(b)) mainly consist of S 3s of the LaS subsystem. The next four bands of S 3s of the LaS subsystem (II in figure 6(b)) are mixed with S 3s states of some of the sulphur atoms of the NbS_2 subsystem. The S 3s bands of the NbS_2 subsystem are divided into two separate parts. 12 bands (III in figure 6(b)) of the S 3s of NbS_2 subsystem are mixed with S 3s of the LaS subsystem, which indicates strong interlayer interactions. However, this hybridization does not contribute to net interlayer bonding, because all bonding and antibonding states are occupied. The other 16 bands (IV in figure 6(b)), lying at the lowest energy range, form a separate part, with bonding and antibonding states, and consist of only S 3s states of the NbS_2 subsystem. The S 3s bands show very little dispersion along the Γ-Y and T–Z directions parallel to the $\boldsymbol{k}_y$ axis (interlayer). This is understandable because, in the directions parallel to $\boldsymbol{k}_y$, the S–S distances are too long for strong interlayer 3s–3s interactions. The S 3s bands of the LaS subsystem have a dispersion of about 0.5 eV along the Γ–Z direction, which is of the same order as in LaS [20]. It is remarkable that the S 3s bands of the LaS subsystem have a very small dispersion along the X–Γ and A–Z directions parallel to $\boldsymbol{k}_x$, while the S 3s bands of the NbS_2 subsystem have a dispersion parallel to $\boldsymbol{k}_x$ as large as those in the Γ–Z directions.

The bands near the Fermi level show a strong anisotropy. There is a large dispersion (about 0.5–1.0 eV) for directions with a $\boldsymbol{k}$ component perpendicular to $\boldsymbol{k}_y$. This dispersion is caused by strong intralayer interactions in the subsystems and is also found in the band structures of the components. Near the Fermi level the bands have a small dispersion of about 0.01–0.05 eV in the interlayer ($\boldsymbol{k}_y$) direction (Γ–Y and T–Z). Below the Fermi level

some of the bands show a dispersion of about 0.3 eV in the interlayer direction, which is smaller than in the misfit layer compounds $(SnS)_{1.17}NbS_2$ and $(SnS)_{1.20}TiS_2$ [4, 5]. The bands across the Fermi level along the Γ-X direction have mainly Nb $4d_{z^2}$ character and have a dispersion as large as along the Γ–Z direction. Therefore the anisotropy between the *a* and *c* directions is very small.

4. Photoemission spectra measurements

The misfit layer compound $(LaS)_{1.14}NbS_2$ was synthesized and crystals were grown by vapour transport as described before [7]. The crystals obtained were approximately squares with rounded sides, with dimensions of about 5–10 mm. We carried out XPS measurements in a small-spot ESCA machine from Vacuum Generators. A spot diameter of 300–600 μm was used. The radiation source was an Al anode using the K α line with a photon energy of 1486.6 eV. The sample surface was cleaned by stripping with Scotch tape in the preparation chamber at a base pressure of 10^{-9} Torr. The sample with a fresh surface was transported to the main chamber (base pressure, 10^{-10} Torr). We also performed UPS measurements with photons of energy 21.2 eV from a helium lamp.

Figures 8(a), 8(b) and 8(c) show the x-ray photoelectron spectra of the core electrons La 3d, Nb 3d and S 2p, respectively. The latter two are compared with the corresponding x-ray photoelectron spectra of the misfit compound $(SnS)_{1.17}NbS_2$ [4, 23]. There is no significant shift in the Nb core levels. However, the spectra of the S 2p core levels in $(LaS)_{1.14}NbS_2$ have an approximately 0.8 eV higher binding energy than in $(SnS)_{1.14}NbS_2$ (table 7). This shift also exists in spectra of the S 2s core electrons. Such a shift is presumably due to strong ionic interactions of La with S atoms in both the LaS and the NbS_2 layers.

Table 7. Bonding energies and full widths at half maximum (in parentheses) of the measured core level electrons of the misfit layer compounds $(LaS)_{1.14}NbS_2$, $(SnS)_{1.17}NbS_2$ and 2H-NbS_2.

	$(LaS)_{1.14}NbS_2$ (eV)	$(SnS)_{1.17}NbS_2$ (eV)	2H-NbS_2 (eV)
S 2s	225.6 (2.7)	225.2 (2.1)	
S $2p_{1/2}$	162.8 (0.9)	161.9 (0.8)	
S $2p_{3/2}$	161.5 (1.5)	160.8 (1.2)	
Nb $3p_{1/2}$	377.2 (2.2)	377.3 (2.8)	377.3 (2.8)
Nb $3p_{3/2}$	361.7 (3.1)	361.9 (3.1)	361.9 (3.1)
Nb $3d_{3/2}$	206.5 (1.2)	206.2 (2.0)	206.3 (2.0)
Nb $3d_{5/2}$	203.5 (0.9)	203.3 (1.6)	203.5 (1.6)
La $3d_{3/2}$	850.8 (3.5)		
	854.5 (2.0)		
La $3d_{5/2}$	834.0 (3.2)		
	837.7 (1.9)		
La $4d_{3/2}$	105.4 (2.2)		
	108.0 (2.0)		
La $4d_{5/2}$	102.3 (2.6)		
	104.4 (2.3)		

The x-ray photoelectron spectra of the La 3d and 4d core levels are more complex. Figure 8(a) and table 7 show that there are two sets of peaks for the La 3d levels. The peaks at 850.8 and 854.5 eV are for the La $3d_{3/2}$ core level and the peaks at 834.0 and 837.7 eV are for La $3d_{5/2}$ core levels. The ratio $I(3d_{3/2})/I(3d_{5/2})$ of the intensities is about

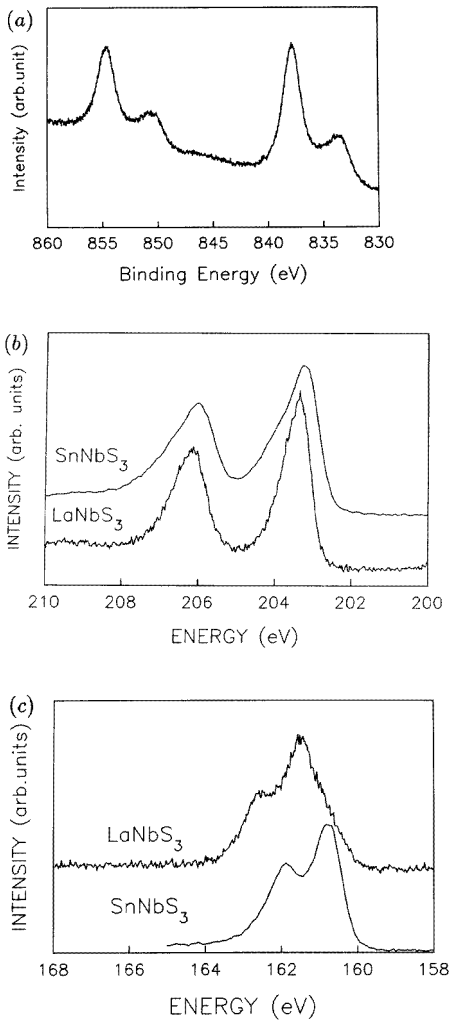

Figure 8. X-ray photoelectron spectra of the core level electrons for $(LaS)_{1.14}NbS_2$ and $(SnS)_{1.17}NbS_2$: (a) La 3d; (b) Nb3d; and (c) S2p.

4/6, corresponding to the occupation numbers of $3d_{3/2}$ and $3d_{5/2}$ states. The intensity ratio for La $3d_{3/2}$ (or La $3d_{5/2}$) of the peak at higher energy to that at lower energy is about 3/1. The energy splitting of the peaks is about 3.8 eV. A splitting of this type is observed for all La compounds and is ascribed to the many-body effects [24–26].

The band-structure calculations show that the La 4f orbitals are seen above the Fermi level. Therefore the ground state is La $4f^{\circ}$. X-ray absorption spectra of the La $3d_{5/2}$ to La $4f_{7/2}(M_5)$ transition also showed that the La 4f states are empty [27]. However, in the final state of the La 3d photoemission, the La 4f level is pulled below the Fermi level by the attractive potential of the core hole. As a consequence there are two final states, a screened state with $3d^9 4f^1 \underline{L}$ configuration, with a ligand hole $\underline{L}$, and an unscreened state with $3d^9 4f^0$ configuration. Therefore, photoemission in the two peaks corresponds to final states $3d^9 4f^0$ (the main peak with a higher binding energy) and $3d^9 4f^1 \underline{L}$ (the satellite with a

lower binding energy). The satellite peak is broader owing to the multiplet interactions. The x-ray absorption spectroscopy peak of the La $3d_{5/2}$ has a binding energy of 834.2 eV [27]. The final state in the La 3d x-ray absorption spectrum is $3d^9 4f^1$, just as the XPS satellite, but the XAS peak is shifted with respect to the XPS satellite as a result of many-body interactions and different selection rules in XAS and XPS [25]. The relative positions of the XAS peak and the XPS satellite for $(LaS)_{1.14}NbS_2$ are very similar to what is observed for La metal [25].

The splitting ΔE between the XPS main line (indicated by subscript m) and satellite (indicated by subscript s), and the intensity ratio I_m/I_s can be described with a simple model, involving the hybridization T between La 4f and the ligand orbitals (S 3p) [24]. The equations are $\Delta E = \sqrt{(\Delta - U_{fc})^2 + 4T^2}$, $I_m/I_s = 1/\tan^2\theta$ and $\tan(2\theta) = 2T/(\Delta - U_{fc})$, where Δ is the difference between the energies of La 4f and the ligand orbital in the initial state, and U_{fc} is the Coulomb interaction between a La 4f electron and the 3d core hole. With the observed values $\Delta E = 3.8$ eV and $I_m/I_s = 3$ we obtained $U_{fc} - \Delta = 1.9$ eV and $T = 1.6$ eV. The La 4f state is calculated at about 4 eV above the Fermi level. However, because the local-density approximation gives an energy for unoccupied La states which is about 5 eV too low, a more realistic value for the energy of La 4f is 9 eV above the Fermi level. The S 3p states are at about 3 eV below the Fermi level (figure 7), so that $\Delta \simeq 12$ eV. Using $U_{fc} - \Delta = 1.9$ eV we find that $U_{fc} \simeq 14$ eV. The values $U_{fc} \simeq 14$ eV and $T = 1.6$ eV are comparable with the values obtained for other La compounds with more elaborate calculations, taking into account also the multiplet splitting and the ligand band width [26, 28, 29].

The x-ray photoelectron spectrum of the valence band of the misfit layer compound $(LaS)_{1.14}NbS_2$ is shown in figure 9. A calculated spectrum is obtained from the partial DOS by multiplying by the appropriate cross section for photoemission (for XPS with a photon energy of 1486.6 eV, the cross sections are 0.000 76 for La 5d, 0.0019 for S 3s, 0.0010 for S 3p and 0.0026 for Nb 4d [30]. The S 3s band of the spectra is quite wide and ranges from about -16 eV to about -10.0 eV. The maximum is situated at about -13.2 eV which agrees quite well with the strong peak of the calculated spectrum (-13.2 eV of S(Nb) 3s). However, the S 3s peak of the LaS subsystem (about -11.9 eV), which is visible in UPS, is not clearly visible in XPS because it is calculated to be weaker than the S 3s peak of NbS_2 and because of the resolution (about 1.0 eV). The XPS valence band begins at -8.0 eV. The broad peak from -8.0 to -1.5 eV is mainly S 3p mixed with some La 5d and Nb 4d states. There is a narrow peak (about 1.5 eV) just below the Fermi level which corresponds mainly to Nb $3d_{z^2}$ states. Considering the resolution of the measurements (about 1.0 eV for this case) the calculated bands are in good agreement with the experimental data.

Figure 10 shows the ultraviolet photoemission spectrum of the valence band of $(LaS)_{1.14}NbS_2$. The UPS data correspond quite well to the XPS results, but the resolution is much better. The first sharp peak below the Fermi level is again the Nb $4d_{z^2}$ band; it has a width of about 1.5 eV, which is larger than for $(SnS)_{1.17}NbS_2$. This is due to a larger band filling in $(LaS)_{1.14}NbS_2$. The band-structure calculations show that charge transfer from the MS subsystem to the NbS_2 subsystem is about 0.7–0.8 electrons per T atom for M = La; it is about 0.3 electrons per T atom for M = Sn [4]. The S 3s band is quite broad (from -15.5 eV to -11.5 eV) and has a broad peak with some structure, which corresponds to several S 3s bands of the LaS and NbS_2 subsystems. The Nb 4d band has a lower intensity than expected from the calculation (the cross section is 22.10 for Nb 4d and 4.33 for S 3p) [30]. The shape of the S 3p band is more like that of the LaS than of the NbS_2 part. Because UPS is more surface sensitive than UPS, this could be due to a surface layer of LaS rather than NbS_2.

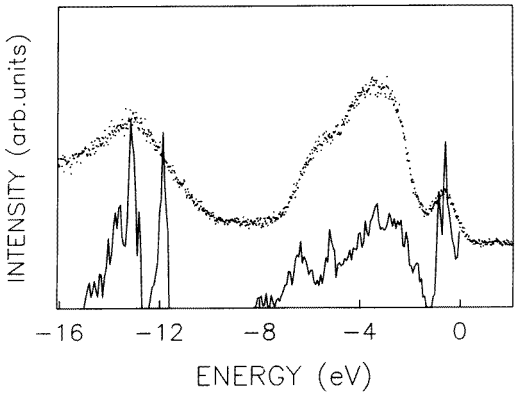

Figure 9. X-ray photoelectron spectrum of the valence band of $(LaS)_{1.14}NbS_2$ (dots), compared with the calculated results.

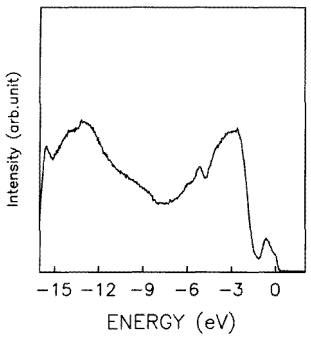

Figure 10. Ultraviolet photoelectron spectrum (photon energy, 21.2 eV) of the valence band of $(LaS)_{1.14}NbS_2$.

5. Discussion

From these band-structure calculations it is seen that in $(LaS)_{1.14}NbS_2$ there is a transfer of about 0.7 electrons per Nb atom from the LaS layers to the NbS_2 layers. The bond valence calculations show that the interlayer La–S(NbS_2) bonds are quite strong (interlayer bond valence is about 0.8–0.9 per La atom) (this is also the case in other rare-earth-based misfit layer compounds [3]), indicating that there are strong bonds between the two subsystems. The interlayer energy dispersion is about 0.3 eV, slightly smaller than in the misfit layer compounds $(MS)_{1+x}TS_2$ (M = Sn; T = Ti or Nb) [4, 5]. Near the Fermi level the interlayer energy dispersion is about 1.0 eV, while the interlayer dispersion is very small, about 0.05 eV. The Fermi level is in the middle of the Nb $4d_{z^2}$ bands, which means that the electrical transport properties are mainly determined by the Nb $4d_{z^2}$ states.

This dispersion of the S 3s bands in the Γ–Z direction of the LaS subsystem (about 0.5 eV) is smaller than that of the S 3s bands of the NbS_2 subsystem (about 1.0 eV). Along the Γ–X direction (the incommensurate direction), the dispersion of S 3s of the LaS subsystem is even smaller. This small dispersion may be related to a strong ionic contribution in the bonding, and a possible localization of La 5d electrons. Such a

localization induced by the incommensurate structure was suggested by Suzuki *et al* [31].

An interesting question concerns the origin of the stability: what is the nature and strength of the interlayer bonding? For the transition-metal dichalcogenides the interlayer bonding is due to weak van der Waals interactions. In alkali-metal intercalates A_xTX_2 the interlayer interaction is mainly due to the electrostatic interaction between the positively charged A^+ ions and the negatively charged TX_2^- layers. In the misfit layer compounds $(MX)_{1+x}TX_2$ (M = Sn or Pb; X = Se or S) there is a small charge transfer (about 0.2–0.3 electrons per T atom) from the MX to the TX_2 layers and the stability is dominated by covalent interlayer bonds between the M atoms and S atoms of the TS_2 subsystem [4, 5]. In the rare-earth-element-based misfit layer compounds there is a large charge transfer (e.g. about 0.7 electrons per Nb atoms) and strong interlayer bonds (e.g. La–S(NbS_2) with bond valence 0.8–0.9 vu per La atom).

From a comparison of the calculated band structure of $(LaS)_{1.14}NbS_2$, LaS and NbS_2 we concluded that there is a transfer of about $\Delta n \simeq 0.7$ electrons per Nb atom from LaS to the NbS_2 subsystem. This charge transfer leads to a charge of $0.7e$ for the LaS layers, and a charge of $-0.7e$ for the NbS_2 layers (charges per formula unit $(LaS)_{1.14}NbS_2$. The electrostatic interlayer bonding will be of the order of $\Delta E(\text{interlayer}) \simeq (e\Delta n)^2/\epsilon d$, where d is the distance between the midplanes of the layers ($d = b/4$), and ϵ is an effective dielectric constant which takes into account the screening of the interactions. If we use for ϵ the value $\epsilon_\infty \simeq 8$ (smaller than the value of $\epsilon = 10$ for $(SnS)_{1.17}NbS_2$) [32, 33], we obtain $\Delta E(\text{interlayer}) \simeq 0.10$ eV/formula unit; without screening ($\epsilon = 1$) we find that $\Delta E(\text{interlayer}) \simeq 0.6$ eV. The electrostatic binding energy of $(LaS)_{1.14}NbS_2$ is much larger than that of $(SnS)_{1.17}NbS_2$ [4].

The cohesive energy of LaS can be obtained from

$$E_{coh}(\text{LaS}) = -\Delta H_f^0(\text{LaS}) + H_0(\text{La}) + H_0(\text{S}).$$

where ΔH_f^0(LaS) is the standard heat of formation of LaS from the elements, and H_0(La) and H_0(S) are the heat of formation of gaseous atoms La and S, respectively, from the elements in their standard states. With the values $H_0(\text{La}) = 4.48$ eV, $H_0(\text{S}) = 2.88$ eV and $\Delta H_f^0(\text{LaS}) = -4.73$ eV) [34], we obtain $E_{coh}(\text{LaS}) = 12.01$ eV. In LaS, each La atom is coordinated by six sulphur atoms, and the valence of La is three, so that the bond valence of one La–S bond in LaS is $(\frac{1}{6}) \times 3 = \frac{1}{2}$. We assume that the binding energy of a La–S bond with bond valence V_i is $V_i E_0$ and $6 \times (\frac{1}{2})E_0 = 12.0$ eV, so that $E_0 = 4.0$ eV. The bond valence contribution of the interlayer bonds is about $V_b = 0.9$ (see table 2). Therefore the interlayer bonding energy per La atom, $\Delta E(\text{interlayer}) = V_b E_0 = 3.6$ eV, which is much larger than in $(SnS_{1.17}NbS_2$ or $(PbS)_{1.18}TiS_2$ [4]. We estimated for the electrostatic interlayer energy due to charge transfer a value between 0.1 and 0.6 eV/formula unit. We conclude that the contribution of the La^{3+}–S^{2-}(NbS_2) interlayer interaction is considerably larger than the electrostatic interaction as calculated above.

$(LaS)_{1.14}NbS_2$ has p-type metallic electronic conduction, with a hole concentration of about 0.10 holes per Nb atom deduced from Hall effect measurements with the simple relation $R_H = (pe)^{-1}$ [35, 36]. The optical reflectivity showed that there are about 0.3 holes per Nb atom (32, 33]. These data agree with the band-structure calculations (about 0.3 holes per Nb atom). The electrical resistivity measurement showed a large resistivity ratio ρ_c/ρ_{ab} (about 50 [35]), which can be explained by the small dispersion in the interlayer direction of the band at the Fermi energy. The residual electrons in the LaS layers (about 0.4 electrons per La atom) are probably in La 5d orbitals. The La 4f states are empty and far above the Fermi level, which agrees with XPS and XAS measurements [27]. The rare-earth misfit layer compounds are mechanically harder than the Sn-, Pb-, Bi- and Sb-based misfit

compounds which is explained by the strong interlayer bonds.

Acknowledgments

We are very grateful to Mr J Baas for the growth of large single crystals. We would like to thank Mr A Heeres for kind help with the XPS and UPS experiments.

References

[1] Wiegers G A and Meerschaut A 1992 *Incommensurate Sandwiched Layered Compounds (Mater. Sci. Forum 100–1)* ed A Meerschaut A (Hedersmannsdorf: Trans Tech) pp 101–72
[2] van Smaalen S 1992 *Incommensurate Sandwiched Layered Compounds (Mater. Sci. Forum 100–1)* ed A Meerschaut A (Hedersmannsdofr: Trans Tech) pp 173–222
[3] Wiegers G A 1996 *Progress in Solid State Chem.* **24** 1–139
[4] Fang C M, Ettema A R H F G, Wiegers G A, Haas C, van Leuken H and de Groot R A 1995 *Phys. Rev.* B **52** 2336
[5] Fang C M, Wiegers G A, Haas C and de Groot R A 1996 *J. Phys.: Condens. Matter* **8** 1663
[6] Meerschaut A, Rabu P and Rouxel J 1989 *J. Solid State Chem.* **78** 35
[7] Wiegers G A, Meetsma A, Haange R J, van Smaalen S, de Boer J L, Meerschaut A, Rabu P and Rouxel J 1990 *Acta Crystallogr.* B **46** 324
[8] van Smaalen S 1991 *J. Phys.: Condens. Matter* **3** 1247
[9] Petricek V, Maly K and Cisarova I 1991 *Methods of Structural Analysis of Modulated Structures and Quasicrystals* ed J M Perez-Mato, F J Zuniga and G Madariaga (Singapore: World Scientific)
[10] Rouxel J, Moêlo R, Lafond A, DiSalvo F J, Meerschaut A and Roesky R 1994 *Inorg. Chem.* **33** 3358
[11] Lafond A, Deudon C, Meerschaut A and Sulpice A 1994 *Eur. J. Solid State Inorg. Chem.* **31** 967
[12] Ren Y, Baas J, Meetsma A, de Boer J L and Wiegers G A *Acta Crystallogr.* B at press
[13] Hahn T (ed) 1983 *International Tables for Crystallography* vol A (Dordrecht: Reidel)
[14] Brown I D and Altermatt D 1985 *Acta Crystallogr.* B **41** 244
[15] Brese N E and O'Keefe M 1991 *Acta Crystallogr.* B **47** 192
[16] Bergman H (ed) 1983 *Gmelin Handbook of Inorganic Chemistry, Sc, Y, La–Lu (Rare Earth Elements), System Number 27, c7: Sulfides* (Berlin: Springer)
[17] van Leuken H, Lodder A, Czyzyk M T, Springelkamp F and de Groot R A 1990 *Phys. Rev.* B **41** 5613
[18] Williams A R, Kübler J and Gelatt C D Jr 1979 *Phys. Rev.* B **19** 6094
[19] Hedin L and Lundqvist B I 1971 *J. Phys. C: Solid State Phys.* **4** 2064
[20] Lu Z W, Singh D J and Krakauer H 1988 *Phys. Rev.* B **37** 10 045
[21] Czyzyk M T and Sawatzky G A 1994 *Phys. Rev.* B **49** 14 211
[22] Doni E and Girlanda R 1984 *Electronic Structure and Electronic Transitions in Layered Materials* ed V Grasso (Dordrecht: Kluwer)
[23] Ettema A R H F and Haas C 1993 *J. Phys.: Condens. Matter* **5** 3817
[24] van der Laan G, Westra C, Haas C and Sawatzky G A 1981 *Phys. Rev.* B **23** 4369
[25] Esteva J M, Karnatak R C, Fuggle J C and Sawatzky G A 1983 *Phys. Rev. Lett.* **50** 910
[26] Kotani A, Okada M, Jo T, Bianconi A, Marcell A and Parlebas J C 1987 *J. Phys. Soc. Japan* **56** 798
[27] Ikeda T, Okada K, Ogasawara H and Kotani A 1990 *J. Phys. Soc. Japan* **59** 622
[28] Imada S and Jo T 1990 *Phys. Scr.* **41** 15
[29] Ettema A R H F, van Smaalen S, Haas C and Turner T S 1994 *Phys. Rev.* B **49** 10 585
[30] Kohn S E, Yu P Y, Petroff Y, Shen Y R, Tsang Y and Cohn M L 1973 *Phys. Rev.* B **8** 1477
[31] Suzuki K, Kondo T, Enoki T and Bandon S 1993 *Synth. Met.* **55–7** 1741
[32] Ruscher C H, Haas C, van Smaalen S and Wiegers G A 1994 *J. Phys.: Condens. Matter* **6** 2117
[33] Hangyo M, Nishio T, Nakashima S, Ohno Y, Terashima T and Kojima M 1993 *Japan. J. Appl. Phys. Suppl.* **32** 581
[34] *CRC Handbook of Chemistry and Physics* 1991 72nd edn (Boca Raton, FL: CRC)
[35] Terashima T and Kojima N 1992 *J. Phys. Soc. Japan* **61** 3303
[36] Wiegers G A and Haange R J 1991 *J. Phys.: Condens. Matter* **3** 9929